International Journal of Heat and Mass Transfer 52 (2009) 5643–5651

Contents lists available at ScienceDirect

International Journal of Heat and Mass Transfer

journal homepage: www.elsevier.com/locate/ijhmt

Experimental study on flash evaporation from superheated water jets: Influencing factors and formulation of correlation

Sami Mutair [a], Yasuyuki Ikegami [b,*]

[a] Graduate School of Science and Engineering, Saga University, 1-Honjo-machi, Saga City, Saga Prefecture 840-8502, Japan
[b] Institute of Ocean Energy, Saga University, 1-Honjo-machi, Saga City, Saga Prefecture 840-8502, Japan

ARTICLE INFO

Article history:
Received 19 September 2008
Received in revised form 6 February 2009
Accepted 1 May 2009
Available online 31 July 2009

Keywords:
Flash evaporation
Superheated jet
Correlation
Sigmoid model
Desalination

ABSTRACT

This paper reports on the influencing factors and their effects on the intensity of flash evaporation that occurs in the superheated water jets. A variety of experiments were conducted and four variables were investigated namely velocity of flow, initial temperature, superheat degree and injection nozzle diameter. An exponentially decaying curve model that predicts temperature variation at the centerline of the upward flowing jet was proposed and employed in the demonstration of the nature of influence of each experimented variable. Evaporation end height was estimated and correlated by an empirical equation; this equation is thought to be useful in designing the flash evaporation chamber.

1. Introduction

Water issue and the securing of sustainable water supply have always received considerable interest from researchers and governments likewise due to its necessity for the existence of mankind. Desalination of seawater has proven its sustainability in the substitution of fresh water shortage. However, due to the rapid increase of energy cost in addition to the environmental problems accompanying the combustion of fossil fuels in the conventional desalination processes, the need for the development of sustainable and environment-friendly techniques that utilize the renewable energy resources in the desalination of seawater has arisen. Utilizing the thermal energy of the ocean in driving the desalination process is one of the promising solution techniques in which the available temperature difference between the surface and the deep layers of the ocean is utilized in the desalination of seawater by evaporating the warm surface water in a depressurized chamber and recondensing the generated steam on a surface condenser, that is supplied with the cold seawater from the deep layers of the ocean. As the available ocean thermal energy is of low grade, and heat is to be exchanged between sources of relatively low temperature difference, an efficient heat transfer processes should be adopted.

Flash evaporation from superheated liquid jets have received considerable attention due to its high efficiency and dispensability of the heat exchange surfaces which consume a major part of the total system expenses, in addition to the associated corrosion, fouling and maintenance problems. However, deep understanding of the flash evaporation phenomenon that occurs in the superheated jets and the characteristics of the flashing jets are vital for the design of the flash evaporation chamber.

Several works that report on flash evaporation from superheated water jets as a means of low-temperature desalination were conducted. Sasaki et al. [1] studied this phenomenon and classified the flow of the jet into four different patterns based on the velocity of flow and the degree of superheat. Miyatake et al. [2,3] experimentally investigated the flash evaporation phenomenon that occurs in the superheated water jets of different thicknesses flowing downward at initial liquid temperature that ranges from 40 to 80 °C and several nozzle diameters. Correlation of temperature variation at the centerline of the jet was carried out over the experimented range of variables. However, Uehara et al. [4] conducted experiments on flash evaporation in superheated jets at initial liquid temperature of about 30 °C and showed that correlations proposed in [3] are not applicable when liquid temperature is less that 40 °C. Ikegami et al. [5] investigated the influence of the flow direction on flash evaporation intensity and showed that the upward flowing jets evaporate faster than those flowing downward. Furthermore, Brown and York [6] studied the mechanism of spray formation by the flashing of cylindrical jets of both water and Freon-11 and the spray formed by this process; analysis for drop sizes, drop velocities, and spray patterns was carried out with the assistance of the high speed photography of the breakup zone and of the spray, with drop sizes and velocities computed from a photographic analytical procedure, where most of the data were collected for superheated water

* Corresponding author. Tel.: +81 952 28 8624; fax: +81 952 28 8595.
E-mail address: ikegami@ioes.saga-u.ac.jp (Y. Ikegami).

0017-9310/$ - see front matter © 2009 Published by Elsevier Ltd.
doi:10.1016/j.ijheatmasstransfer.2009.05.009

injected into the room atmosphere. A critical superheat was found, above which the jet of liquid is shattered by rapid bubble growth within it. Duan et al. [7] numerically investigated the effect of superheat degree on the extinction length of flashing jets; the range of superheat degree was from 77 to 231 °C, the injection and back pressure were kept constant at 17 and 0.2 MPa, respectively. They found that jet extinction length decreases with the increase of superheat degree due to the increase of evaporation rate. Their finds compared with the experimental results obtained by Simoes-Moreira et al. [8] using liquid *iso*-octane showed consistency. Vieira and Simoes-Moreira [9] experimentally examined the flashing phenomenon in liquid iso-octan emerging at very high injection-to-discharge pressure ratios from a conical converging nozzle having an exit diameter of 0.31 mm. According to their analysis performed using two visualization techniques (schlieren and back-lighting) methods, flashing was found to take place on the surface of the liquid core through an evaporation wave process; moreover, through the photographs of the liquid core taken at very low backpressure conditions, it has been inferred that no phase transition or nucleation sites were observed in the liquid jet at the exit plane of the nozzle. On investigating the influence of initial liquid temperature on the extinction length of the jet, it was shown that this length decreases in an exponential trend as the injection temperature increases.

However, works that report on the characteristics of temperature variation in superheated flashing water jets are few, and the influence of flow conditions and size of injection nozzle is not clarified thoroughly. Furthermore, temperature variation within the superheated jet after being injected into the depressurized environment has always been investigated as time dependent assuming the flow velocity is either constant [2,3] or gravity-governed motion and neglecting the interfacial drag that originates between the two phases [10]. To overcome this inadequacy arising from these assumptions, temperature variation within the superheated jet is investigated in this paper with reference to travelled distance. While most of the works reported in the literatures concerning flash evaporation were done on very small nozzles and highly superheated liquids, this work reports on numerous carefully conducted experiments on flash evaporation from jets of large diameters at relatively low superheat degrees to investigate the influence of flow velocity, initial water temperature, superheat degree and injection nozzle diameter on the characteristics of temperature variation profiles at the centerline of the superheated jet. Several models were applied to simulate the experimental data of temperature decay at the centerline of the jet. Among the investigated models, a sigmoid one that decays exponentially was found appropriate. The proposed model was employed and enabled the demonstration of the nature of influence of each experimented variable.

2. Description of phenomenon

Thermodynamically, flash evaporation occurs when a liquid undergoes a sudden reduction in the surrounding pressure so that the liquid crosses the bubble-point curve and therefore becomes superheated. As a result, part of the liquid immediately turns to vapor to regain equilibrium. Under adiabatic conditions, the generated vapor receives its latent heat of vaporization at the expense of the surrounding liquid and both the vapor and the residual liquid are cooled to the saturation temperature at the reduced pressure. In this research, tap water was injected vertically upward in a depressurized chamber through a set of round straight nozzles at various flow conditions; nucleation occurs at the active nucleation sites formed naturally by the turbulent mixing effects within the jet in addition to the small cavities that exist at the inner nozzles surface with no attempts to induce swirl or nuclei in addition to that acquired ordinarily by flow. However, jets at superheat as low as 1 °C reported partial shattering while at high degrees of superheat, bubble formation and growth starts earlier within the nozzle resulting in greater bubble flow at the nozzle exit and thus, the flow of the formed bubbles intensively shatters the liquid column near the exit into small spray and extends the interfacial area so that evaporation becomes more violent and temperature decline becomes faster. Regardless of the degree of jet shattering, it was found that the water temperature at the centerline of the jet declines in similar manners forming three successive and distinctive zones, each of different characteristics: (1) potential core zone that exists near the nozzle exit and is mainly characterized by un-shattered flow and negligible temperature decline, (2) spray zone through which the jet shatters and diffuses in a conical shape so that the interfacial area extends and the water temperature declines rapidly and (3) Saturation zone through which temperature is so far constant and the equilibrium condition is so far attained. According to the experimental conditions, each of these zones may vary in the initiation point, length and slope of the temperature decline curve within it.

3. Experimental apparatus and procedure

As shown in Fig. 1, water circulates in three separate closed loops, (1) Test water loop in which water is circulated through the heater to be heated up to the desired degree and then injected to the flash chamber maintained at a pressure below the saturation pressure that corresponds to the injected water temperature. As a result, part of the flashing water turns to steam to regain equilibrium and the generated steam is drawn successively to the condenser and the after-condenser due to pressure decline to be condensed and then returned to the flash evaporation chamber again; the non-evaporating part of the flashing water is then drained to the circulation pump to be recycled in the flash evaporation chamber after being heated to the required temperature at the heater. (2) Heating water loop in which water from the hot water reservoir is pumped to the vertical plate type heater and supplies the test water loop by the necessary heat flow. (3) Cooling water loop in which water is pumped from the cold water tank to the vertical plate type condenser and to the shell and tube type after-condenser. Two vacuum pumps connected to the flash evaporation chamber through the condenser and the after-condenser work at full capacity to attain the desired vacuum in the flash evaporation chamber at the beginning of each experiment and then, the vacuum is maintained constant by regulating shut valves. Temperature distribution in the jet is measured in the r–z plane perpendicular to nozzle diameter that divides the jet into two symmetrical halves by 20 platinum resistance thermometers (PRTs) fixed at intervals of 25 mm on a horizontal holding steel bar; the (PRTs) are directed vertically downward facing the jet and the temperature is measured at the lower free end of each (PRT); the holding bar is movable in the z direction and the temperature is measured at 26 stations located at different intervals from 0 to 700 mm starting from the nozzle exit. Fig. 2 shows details of the flash evaporation chamber and Table 1 shows the investigated variables and their experimented range.

The degree of superheat ΔT_s is defined in Eq. (1) while the dimensionless temperature, θ introduced in Eq. (2) indicates the ratio of the superheat degree at a given location, to the initial superheat degree ΔT_s; however, θ will be used to express temperature in the jet throughout this paper.

$$\Delta T_s = T_0 - T_s \tag{1}$$

$$\theta_{(r,z)} = \frac{T_{(r,z)} - T_s}{T_0 - T_s} \tag{2}$$

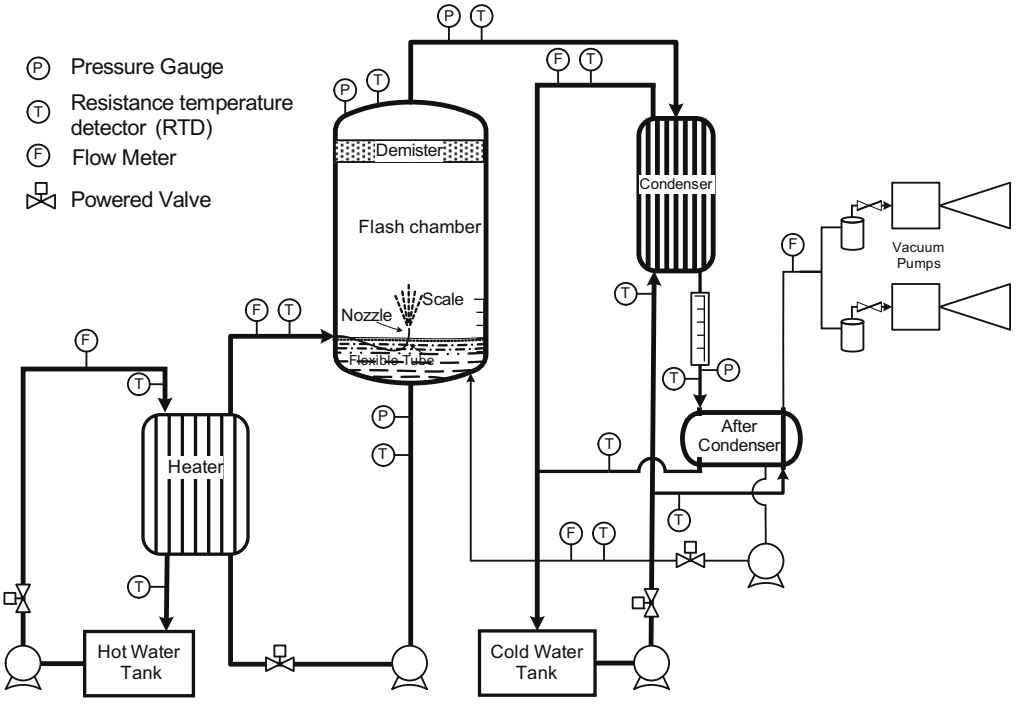

Fig. 1. Layout of experimental apparatus.

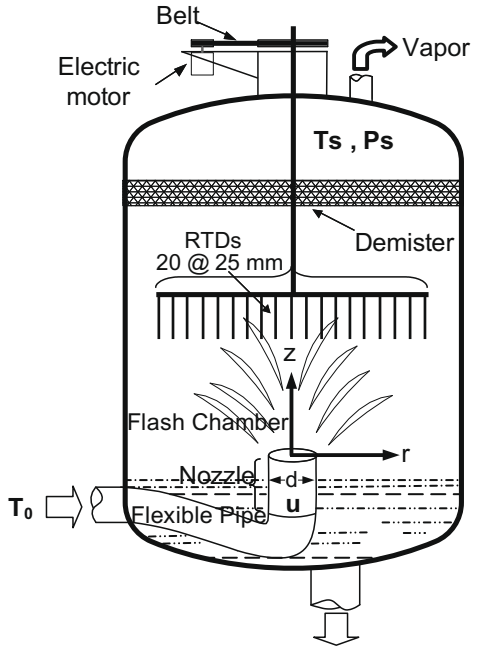

Fig. 2. Details of the flash evaporation chamber.

Table 1
Range of the investigated variables.

Parameter	Experimented range
Nozzle Diameter, d [mm]	54.4, 81.3, 107
Velocity, u [m/s]	0.8, 1.25, 2.21, 3.0, 3.56
Initial temperature, T_0 [°C]	24, 30, 35, 40
Superheat, ΔT_s [°C]	2∼13

where T_0 is initial water temperature measured in the compressed liquid region, T_s is the saturation temperature that corresponds to the pressure inside the flash evaporator, measured at the saturated bulk vapor; z is the vertical distance measured from the nozzle exit level, and r is the radial distance measured from the center of the nozzle.

4. Results and discussion

4.1. Centerline temperature profiles

In order to quantify the effect of the influencing factors on the shape of temperature decline curves, it is necessary to find a reference point on these curves that reflects the variation of these factors. Concerning the selection of a reference point, Bharathan and Penny [10] introduced a dimensionless parameter named effectiveness, ε defined in Eq. (3)

$$\varepsilon = 1 - \left(\frac{T_b - T_s}{T_0 - T_s}\right)_{z=0.8\mathrm{m}} \tag{3}$$

This parameter indicates the ratio of the bulk temperature drop at downstream distance 0.8 m from the nozzle exit, to the initial superheat degree at the inlet, and they investigated the variation of this parameter with the flow velocity of the jet.

Other researchers adopted the value of the centerline dimensionless temperature θ that equals 0.1 as a reference point and considered that the height z at which θ attains this value is sufficient to assume that evaporation is complete. This assumption is justified in spite of the fact that for the evaporation to become complete it is required that θ declines to zero at the end height of the jet. This justification is convincing on the ground that θ has rarely declined to zero through the upward flight of the jet although experiments have shown that the actual amount of produced water is so far equal to the theoretical amount calculated from the heat balance equations. However, evaluation of the height at which θ attains the value 0.1 requires interpolation between the points of higher and lower θ values and this interpolation is so often linear due to the lack of other reliable models that represent the temperature decline curves. The defect of this method is that interpolation is

made between two concerning points and the other readings on the curve are disregarded so that higher errors are expected especially that the value θ equals 0.1 is located in the saturation zone which so often consists of vapor and some water mists of variable temperatures due to the explosive bubble growth accompanied with spraying from the jet. For the aforementioned reasons, temperature readings in this region are unstable and subjected to high uncertainty. Therefore, the need for modeling arises in order to find the height that corresponds to the value of θ equals 0.1 from a suitable model that considers all experimental readings.

Through a variety of experiments, it was observed that water behaves in a similar manner at all investigated conditions and each centerline temperature plot was found to lie on a part of Boltzmann sigmoid curve that decays exponentially. A typical sigmoid curve model is represented by Eq. (4) and drawn in Fig. 3.

$$\theta_0 = A_2 + \frac{(A_1 - A_2)}{\left\{1 + \exp\left[\frac{(z - z_{ip})}{\delta z}\right]\right\}} \tag{4}$$

where θ_0 denotes the dimensionless temperature at the centerline of the jet, A_1 and A_2 are the initial and final values of θ_0, respectively, z_{ip} is the center of curve and also represents the height of the inflection point between the two curvatures of different signs and δz is the approximate range width of z variable within which, θ_0 value changes drastically.

Fig. 4 shows the suitability of the Boltzmann's model for data fitting where the actual distance $z_{(exp)}$ at which the water attains values of θ_0 that ranges from 0.1 to 0.9 for all carried out experiments is plotted on the x-axis against the corresponding distance $z_{(cal)}$ obtained from the proposed sigmoid curve and plotted on the y-axis. At higher values of θ_0, data are matching so well and uncertainty is around 10%. While at θ_0 equals 0.1, the uncertainty is higher. With the knowledge that experimental readings at low values of θ_0 are subjected to high uncertainty, the distance $z_{(cal)}$ at which θ_0 attains the value 0.1 becomes more reliable than $z_{(exp)}$ at the same value of θ_0.

4.2. Influence of experimental variables

As the slope of the curve at any location is an indicator for the local rate of evaporation, location of the curve's inflection point is an object of interest in this study as it implies the highest rate of the flash evaporation, and the variation of experimental conditions reflects strongly on it. The location of the infliction point z_{ip} for each centerline temperature decline curve was calculated from

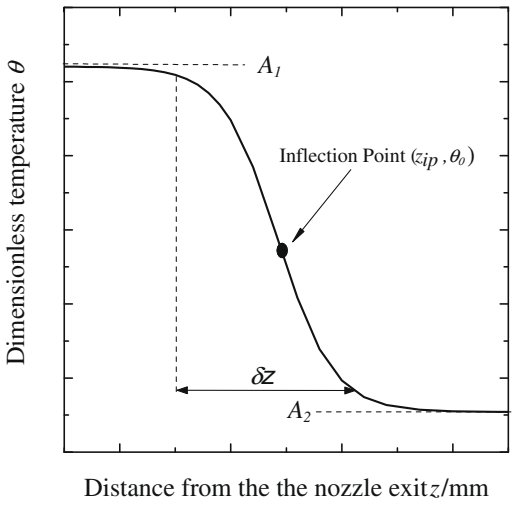

Fig. 3. Typical Boltzmann sigmoid model.

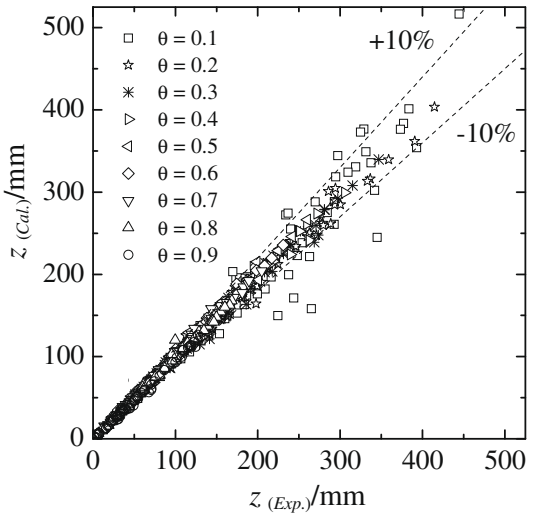

Fig. 4. Experimental and calculated values of the height z at which θ_0 attains several values.

its corresponding sigmoid curve equation obtained by using fitting software. In Fig. 5, the calculated values of the inflection point location $z_{ip(cal)}$ are plotted on the y-axis against the corresponding $z_{ip(exp)}$ values obtained directly from the experimental readings at the equivalent θ_0 values. This figure shows that the inflection point of the simulation curve model $z_{ip(cal)}$ represents the actual inflection point of the experimental readings $z_{ip(exp)}$ with a margin of error around 5%.

4.2.1. Influence of flow velocity

Fig. 6 shows the temperature variation at the centerline of the jet for two sets of experiments carried out at different nozzle diameters of 54.4 and 107 mm. For each set of experiments, temperature variation at the centerline of the jet was plotted at various flow velocities while the other conditions were maintained constant. As shown in this fig., jets of higher flow velocity attain larger θ_0 values at the same downstream distance due to the shorter elapsed time in the depressurized environment. Furthermore, the most significant influence of flow velocity was found to be at short distance from the nozzle exit where the increase of velocity delays

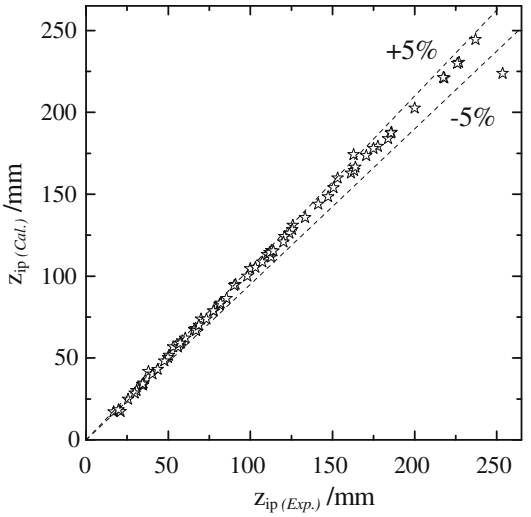

Fig. 5. Uncertainty in the prediction of inflection point location using Boltzmann model.

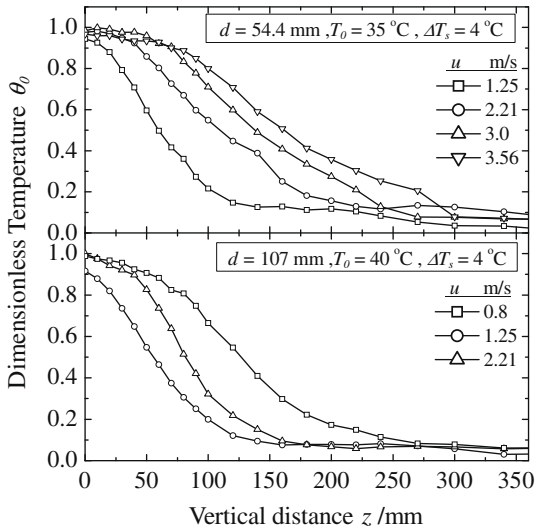

Fig. 6. Centerline temperature profiles at various flow velocities.

the jet disintegration and results in increase of the overall distance required to complete evaporation; this behavior is thought to be attributed to jet inertia which increases with velocity and represents the retarding force that tends to maintain the jet un-shattered so that the coherent liquid column near the nozzle exit extends to longer downstream distance resulting in the increase of the static pressure at the nozzle exit and subsequently, the suppression of the evaporation. Fig. 7 shows the relationship between the flow velocity and the height of each curve's inflection point; the height of inflection point seems to increase in a logarithmic-like relationship with the increase of flow velocity. Bharathan and Penny [10] presented data showing the influence of flow velocity on the variation of water temperature at a vertical distance of 0.8 m form the exit of the vertical spout of 127 mm diameter; they reported that the water temperature was seen to increase slightly with increasing flow velocity up to 1.7 m/s and then decrease once again with further increase of flow velocity. However, the heat flux from the jet was held constant at 210 kW at all the flow velocities; therefore, superheat degree was variable and the reported experimental results might not represent the actual influence of flow velocity when superheat degree is held constant.

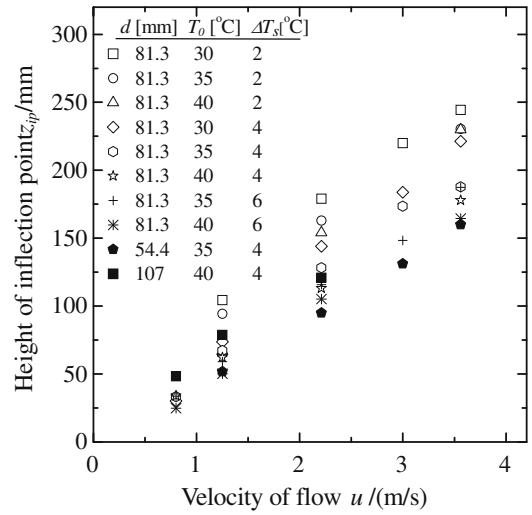

Fig. 7. Variation of the inflection point height with flow velocity.

4.2.2. Influence of initial temperature

An increase of the initial water temperature was found to enhance the flash evaporation which results in shorter length of the potential core zone and reduction of the initial value of θ_0 at the nozzle exit due to bubbling within the nozzle as shown in Fig. 8-a. In Fig. 8-b, which is plotted at higher flow velocity, temperature remains unchanged for a while until a specific distance is elapsed and the bubbling starts at further downstream distance; however, this delay distance decreases with the increase of temperature. For better understanding of influence of temperature, the location of the inflection point z_{ip} is plotted against the initial water temperature at various experimental conditions in Fig. 9. As shown in this figure, the increase of the initial water temperature hastens evaporation and linearly reduces the height of the inflection point. This behavior is thought to be attributed to the decrease of the latent heat of vaporization with the increase of water temperature, whereas the latent heat of vaporization is an interpretation of the energy required to increase the mean separation distance between molecules from the distance in the liquid to that several times larger in the vapor after overcoming the barrier of surface tension. From the microscopic point of view, the volume occupied per molecule in a certain phase is taken to be as the product of the specific volume of that phase times the molecular mass; if we take the cube root of this value as an estimate of the mean spacing of the molecules, then the ratio of the distances between molecules in the two phases L_v/L_l is given by Eq. (5).

$$\frac{L_v}{L_l} = \left(\frac{v_v M/N_A}{v_l M/N_A}\right)^{1/3} = \left(\frac{v_v}{v_l}\right)^{1/3} \tag{5}$$

where L_v and L_l are the mean spacing between molecules in the vapor and liquid phases, respectively; v_v and v_l are the specific volumes of vapor and liquid, respectively; M is the molar mass and N_A is Avogadro's number. Evaluating this ratio at temperatures of 24 and 40 °C implies that the spacing between molecules in the bulk vapor should be 36.26 and 26.25 times that in the bulk liquid at the temperatures 24 and 40 °C, respectively. In addition to the previous argument, for the nucleation process to proceed at nucleation cavity, a certain pressure difference should exist between the inner and outer surface of the bubble embryo to overcome the surface tension forces according to Eq. (6).

$$P_B - P_s = \frac{2\sigma}{r_B} \tag{6}$$

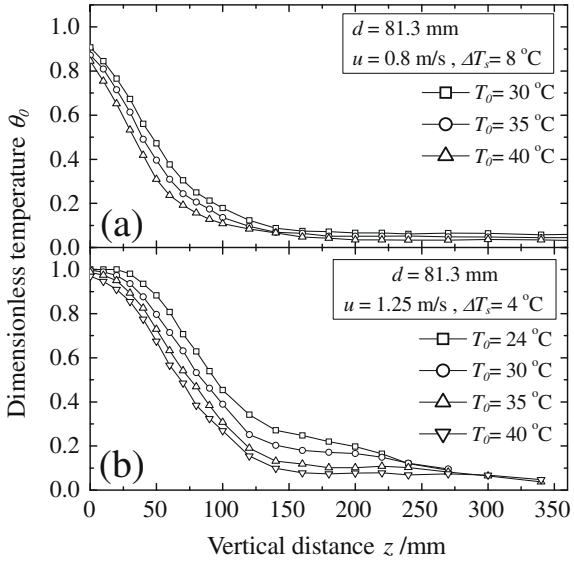

Fig. 8. Centerline temperature profiles at various initial temperatures.

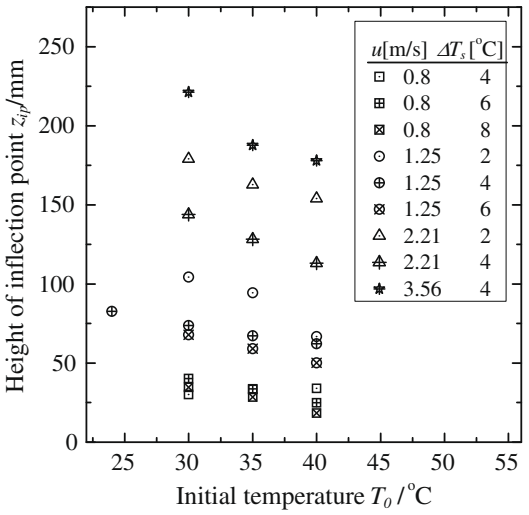

Fig. 9. Variation of Inflection point height with initial temperature.

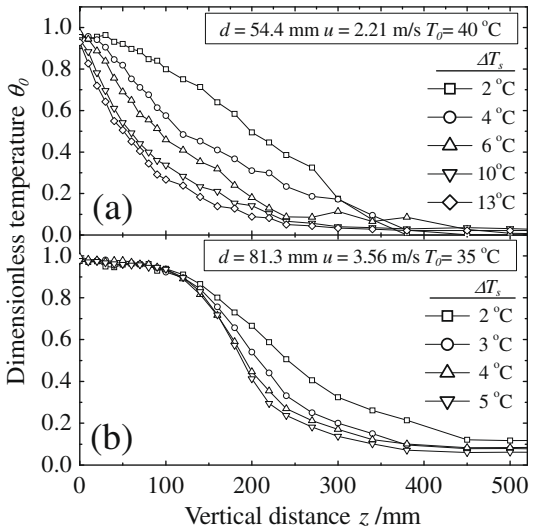

Fig. 11. Variation of θ_0 with distance at various superheat degrees.

where P_B is the inner bubble pressure, P_s is the surrounding liquid pressure (assumed saturation), σ is the surface tension, and r_B is the bubble radius. Referring to Fig. 10, the degree of superheat ΔT_{sat} required to maintain this pressure difference decreases with the increase of the saturation temperature.

4.2.3. Influence of superheat

Fig. 11 shows two sets of temperature profiles at the centerline of the jet obtained at different nozzle diameters, each set is plotted at several degrees of superheat while the other conditions were held constant. As shown in this figure, at relatively low degree of superheat, a certain increase of the degree of superheat results in significant hastening of the flash evaporation and an increase of the slope of the curve particularly in the spray zone and shortens the distance δz through which the majority of sensible heat is consumed by evaporation, while at higher degrees of superheat, the same increment will have less pronounced influence.

Fig. 12 clarifies the nature of the superheat effect, where the vertical distances z at which the water attains values of dimensionless temperature θ_0 from 0.2 to 0.9 were plotted at different degrees of superheat, the curves have steep inclination between the points 2 and 4 of ΔT_s on the x-axis while the trend of curves tends to be horizontal with further increment of superheat degree.

In Fig. 13, the height of each curve's inflection point z_{ip} was plotted against the superheat degrees at various flow conditions; it is shown that the height of the inflection point decreases in an exponential-like relationship with the increase of superheat degree.

The enhancement of flash evaporation by the increase of superheat degree is thought to be attributed to the mean droplet size produced via atomization, whereas it decreases as the degree of superheat increases due to the greater vapor release from the body of the jet; for this reason, degree of superheat is considered the driving force that controls the intensity of flash evaporation.

4.2.4. Influence of nozzle diameter

Fig. 14 shows the effect of nozzle diameter on the temperature profiles at the centerline of the jet for four sets of experiments, the clearest manner in which the nozzle diameter affects the flash evaporation phenomenon is indicated in Fig. 14-a, while the temperature variation profiles in the other sets intersect at several points as shown in Fig. 14-b through d. However, a common behavior in these profiles appears on the value of θ_0 at the nozzle exit, whereas this value increases with the increase of nozzle diameter. This behavior is thought to be attributed to nucleation within

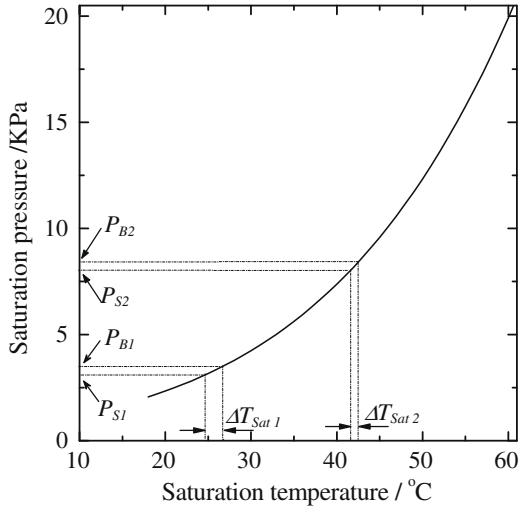

Fig. 10. Variation of the saturation pressure of water with temperature.

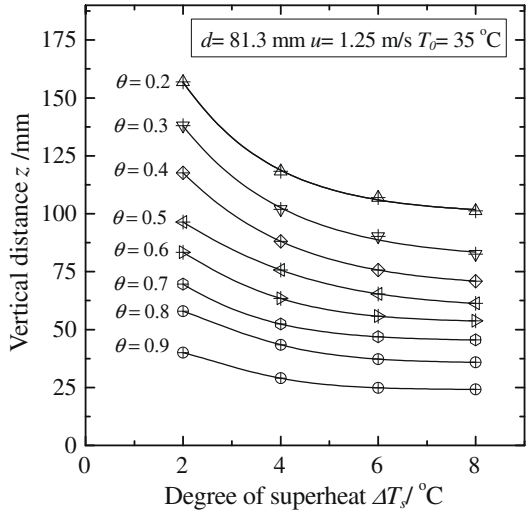

Fig. 12. Relationship between superheat degree and the vertical distance at which θ_0 attains values from 0.2 to 0.9.

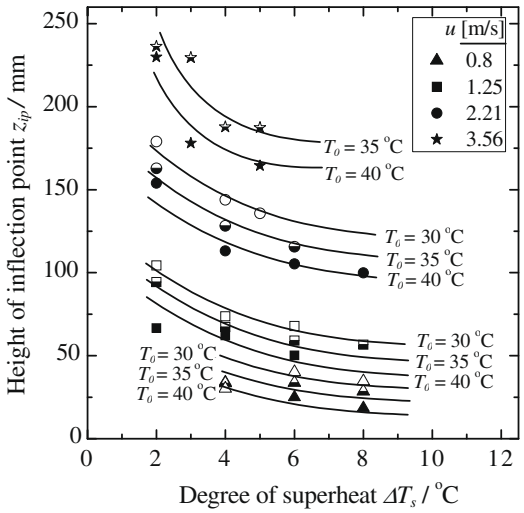

Fig. 13. Variation of the inflection point height with superheat degree.

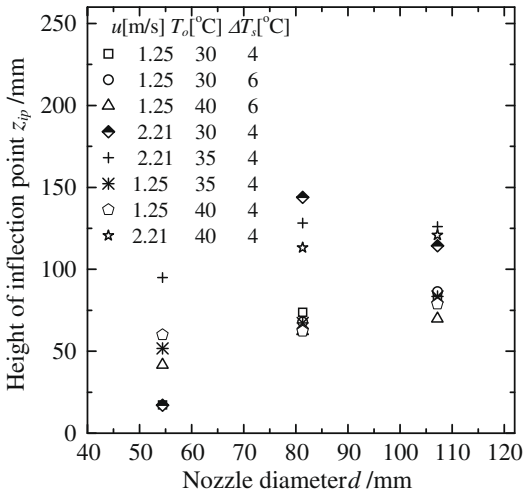

Fig. 15. Influence of nozzle diameter on the height of inflection point.

the nozzle where the ratio of nucleation sites available per unit mass of water is proportional to the reciprocal of nozzle diameter at the same nozzle material and length. Furthermore, nozzle diameter has its effect on the height of the inflection point, as shown in Fig. 15; the height of the inflection point tends to increase with the increase of the nozzle diameter. However, Bharathan and Penney [10] presented experimental data for evaporation from 0.8 m long planar water sheets of various initial thicknesses and flow rates; they demonstrated that evaporation was independent of jet thickness due to shattering effects. Yet, this deduction might not be generalized because jet thickness was found to play a main role in the degree of jet shattering due to the increase of jet inertia with the increase of its diameter; whereas inertia acts as a retarding force that tends to maintain the jet un-shattered.

4.3. Estimation of the inflection point height

Due to its significant importance, attempts were carried out to relate the height of curves inflection point z_{ip} with a suitable group of dimensionless numbers that interpret the flow properties. Among the several candidates, the dimensionless numbers Weber, Froude and Jakob were found most effective. Weber number, *We* defined in Eq. (7) is the ratio of inertia to surface tension forces where ρ and σ are density and surface tension of water, respectively. Froude number, *Fr* defined in Eq. (8) compares inertial and gravitational forces, where *g* is the acceleration of gravity; however, Weber and Froude numbers are strong representatives for the aerodynamic forces which encounter the jet. Jakob number, *Ja* defined in Eq. (9) is the ratio of sensible to latent heat energy absorbed during liquid-vapor

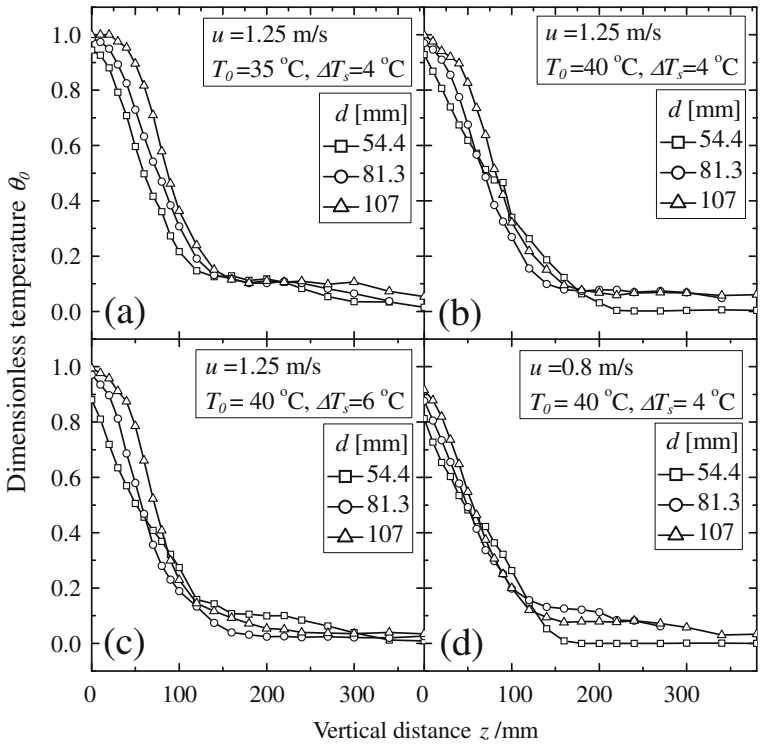

Fig. 14. Influence of nozzle diameter.

phase change and it is a representative of the thermal properties of the water where c_{pl} is the specific heat at constant pressure, and h_{fg} is the latent heat of vaporization.

$$We = \frac{\rho u^2 d}{\sigma} \tag{7}$$

$$Fr = \frac{u}{\sqrt{gd}} \tag{8}$$

$$Ja = \frac{\rho_l c_{pl} \Delta T_s}{\rho_v h_{fg}} \tag{9}$$

Eq. (10) is an empirical arrangement of the above-mentioned dimensionless numbers that estimates the height of inflection point of the temperature decline curve at the centerline of the jet when the experimental conditions are known; regression analysis technique is used and the parameters were arranged to give the best fit of experimental data in a manner that agrees with the nature of influence of each variable. This correlation shows that the inflection point location is governed by both the aerodynamic and thermodynamic qualities of the jet with greater dependence on Froude number as shown in Fig. 16.

$$\frac{z_{ip}}{d} = 0.57 We^{0.19} Fr^{0.71} Ja^{-0.26} \tag{10}$$

4.4. Estimation of the evaporation end height

The height z at which θ_0 declines to the value 0.1 was assumed to be the evaporation end height; however, estimation of this height aims to provide the designers with the nominal height required for the design of the flash evaporation chamber. Performing the same analyses mentioned above, it was observed that Jakob number is of negligible effect on the evaporation end height while it becomes strongly dependent on the aerodynamic properties of the flow represented particularly by Froude number as shown in Eq. (11); variation of the evaporation end height with Froude number is shown in Fig. 17. This correlation implies that, for the flash evaporation to be complete, a certain residence time in the flash evaporation chamber should be elapsed by the flow regardless of its thermal properties.

$$\frac{z_{(\theta=0.1)}}{d} = 1.73 Fr^{0.73} \tag{11}$$

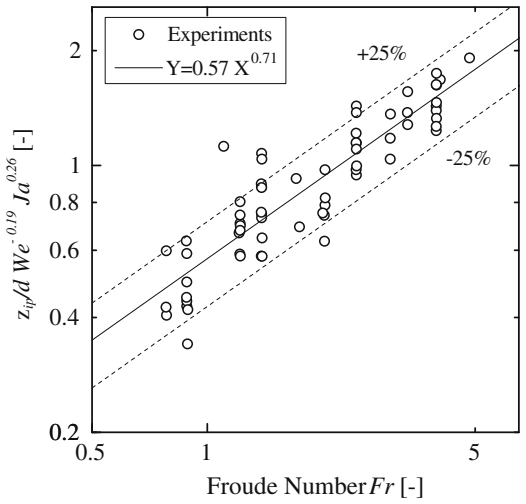

Fig. 16. Dimensionless correlation of the inflection point height.

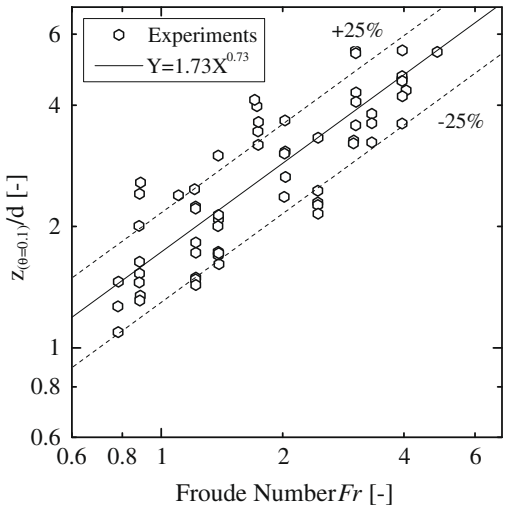

Fig. 17. Dimensionless correlation of the evaporation end height.

5. Conclusion

- Experiments were conducted to investigate the influencing factors and their effect magnitude on the flash evaporation from superheated water jet; these factors include flow velocity, initial water temperature, degree of superheat, and nozzle diameter. The influence of each factor was investigated individually while the other factors were maintained constant.
- Temperature variation at the centerline of the jet was simulated properly by Boltzmann sigmoid model and the location of the curve's inflection point was an object of interest in this study as it implies the highest local evaporation rate, and strongly reflects on the shape of temperature profiles and enables the understanding of the effect of the influencing factors.
- Superheat degree was found to be the driving force of flash evaporation whereas its increase results in faster and more violent evaporation and the level of jet shattering is strongly related to this factor.
- Inflection point and evaporation end heights were normalized with the nozzle diameter and correlated with the dimensionless numbers Weber, Froude and Jacob.
- The obtained results are added to the few available works done on the flash evaporation from large nozzle and give guidance for the design of the flash evaporation chamber.

Acknowledgment

This research is supported by the COE program of Advanced Science and Technology for Utilization of Ocean Energy.

References

[1] H. Sasaki, Y. Ikegami, M. Monde, H. Uehara, Experimental study of flash desalination with upward spray (Flow pattern and temperature distribution), Bull. Soc. Sea Water Sci. Jpn. 59 (5) (2005) 354–360.
[2] O. Miyatake, T. Tomimura, Y. Ide, T. Fujii, An experimental study of spray flash evaporation, Desalination 36 (2) (1981) 113–128.
[3] O. Miyatake, T. Tomimura, Y. Ide, M. Yuda, T. Fujii, Effect of liquid temperature on spray flash evaporation, Desalination 37 (3) (1981) 351–366.
[4] H. Uehara, Y. Ikegami, N. Hirota, Experimental study of spray flash evaporation for desalination and otec, Joint Solar Energy Conference, ASME, 1993, pp. 197–201.

[5] Y. Ikegami, H. Sasaki, T. Gouda, H. Uehara, Experimental study on a spray flash desalination (influence of the direction of injection), Desalination 194 (1–3) (2006) 81–89.
[6] R. Brown, J. Lois York, Sprays formed by flashing liquid jet, AIChE J. 8 (2) (1962) 149–153.
[7] R. Duan, S. Jiang, S. Koshizuka, Y. Oka, A. Yamaguchi, Direct simulation of flashing liquid jets using the MPS method, Int. J. Heat Mass Transfer 49 (2006) 402–405.
[8] J.R. Simoes-Moreira, M.M. Vieira, E. Angelo, Highly expanded flashing liquid jets, J. Thermophys. Heat Transfer 16 (3) (2002) 415–424.
[9] M.M. Vieira, J.R. Simoes-Moreira, Low pressure flashing mechanisms in iso-octane liquid jets, J. Fluid Mech. 572 (2007) 121–144.
[10] D. Bharathan, T. Penney, Flash evaporation from turbulent water jets, J. Heat Transfer 106 (407) (1984).